Sensor-Based Hybrid Position/Force Control of a Robot Manipulator in an Uncalibrated Environment

Di Xiao, Bijoy K. Ghosh, *Fellow, IEEE*, Ning Xi, and T. J. Tarn, *Fellow, IEEE*

Abstract—This paper is devoted to the problem of controlling a robot manipulator for a class of constrained motions. The task under consideration is to control the manipulator, such that the end-effector follows a path on an unknown surface, with the aid of a single camera assumed to be uncalibrated with respect to the robot coordinates. To accomplish a task of this kind, we propose a new control strategy based on multisensor fusion. We assume that three different sensors—that is, encoders mounted at each joint of the robot with six degrees of freedom, a force-torque sensor mounted at the wrist of the manipulator, and a visual sensor with a single camera fixed to the ceiling of the workcell—are available. Also, we assume that the contact point between the tool grasped by the end-effector and the surface is frictionless.

To describe the proposed algorithm that we have implemented, first we decouple the vector space of control variables into two subspaces. We use one for controlling the magnitude of the contact force on the surface and the other for controlling the constrained motion on the surface. This way, the control synthesis problem is decoupled and we are able to develop a new scheme that utilizes sensor fusion to handle uncalibrated parameters in the workcell, wherein the surface on which the task is to be performed is assumed to be visible, but has an a priori unknown position.

Index Terms—Force torque sensor, hybrid control, multisensor fusion, planner, vision system.

I. INTRODUCTION

IT HAS long been recognized that multisensor-based control is an important problem in robotics. As a robot is expected to accomplish more and more complex tasks, such as assembly and task planning in a manufacturing workcell, the need to take advantage of multiple sensors in controlling a system becomes increasingly important. To achieve this end, one proposes to build multisensor-based intelligent robots that can compensate for changes in the environment and uncertainties in the dynamic models without explicit human intervention or reprogramming.

In this paper, we propose a new multisensor-based control strategy to enable the end effector of a robot manipulator track along a class of constrained motions. Concretely, our task is to control the tip of a tool grasped by the end-effector of a robot to follow a curve on an unknown surface, as shown in Fig. 1. Many

D. Xiao is with Fanuc Robotics North America, Inc., Rochester, MI 48309 USA.

B. K. Ghosh and T. J. Tarn are with the Department of Systems Science and Mathematics, Washington University, St. Louis, MO 63130 USA.

N. Xi is with the Department of Electrical Engineering, Michigan State University, East Lansing, MI 48824 USA.
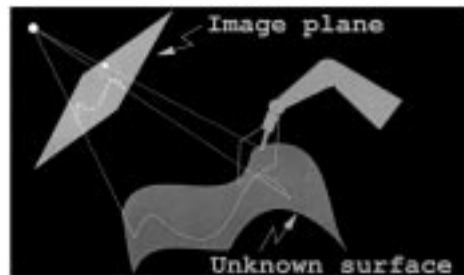
Fig. 1. A typical trajectory-following task with vision and force-torque sensor.

tasks in manufacturing can be characterized in this category, such as welding along a curve, cutting materials and scribing parts, etc. To accomplish the task of moving along a trajectory, it is natural to assume that the trajectory is known. If this is the case, then the problem of following the trajectory is relatively simple. More often, however, the trajectory is on an unknown surface, the position of which is not fixed. To deal with such an uncertainty in the environment, the control system has to rely on reliable information from sensors. As displayed in Fig. 2, we consider three different sensors. They are encoders mounted on each of the six joints of the robot, a force-torque sensor mounted on the wrist of the robot manipulator and a camera fixed to the ceiling of the workcell.

Sensor integration and *multisensor fusion* has been an actively researched area in recent years, as is evident from [1]–[8]. Most of the research has predominantly emphasized the use of sensors providing redundant information. In particular, Nelson and Khosla [18] have proposed an algorithm guided by *resolvability* in order to fuse force and vision. They have proposed to use the two sensors at different stages of the control process while performing the task of *contact transition*, when a manipulator moves in free space and makes contact with a surface.

The control algorithm we propose in this paper utilizes force torque and a visual sensor simultaneously. The force-torque sensor has been used to maintain contact with the surface and to determine the tangent plane to the surface at the point of contact. The visual system has been used to guide the robot arm to follow a trajectory on the surface of contact. The visual system has been used to gain information about the unknown trajectory as well. As is evident in Fig. 2, the proposed control system has a hierarchical structure. The lower level consists of *nonlinear feedback,* which linearizes the input output dynamics of the robot (see [19] for details). The upper level of the control has two parts. The first part is the *planner*, which generates the desired trajectory the end-effector needs to follow, in order to accomplish a task. The second part is the *force controller/position controller* pair that provides the required control signals to
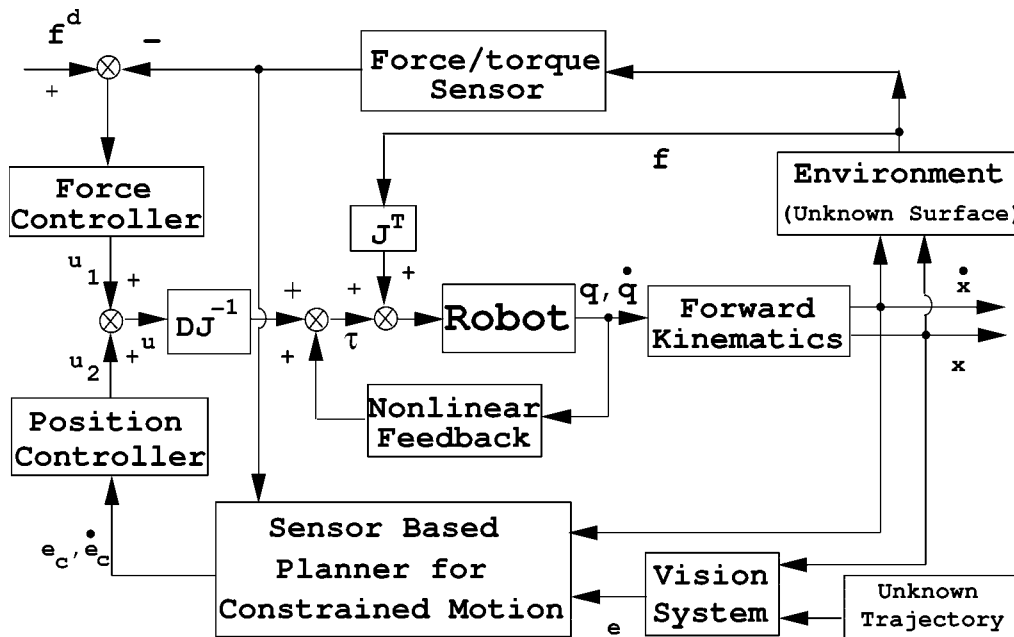
Fig. 2.   Block diagram of the control system with vision and force-torque sensor.

maintain the trajectory generated by the planner. In Fig. 2, the planner has been shown to provide the error signal between the desired trajectory and the estimate of the actual trajectory as provided by the sensors, while the controller pair ensures that the error is driven asymptotically to zero.

This paper is structured as follows. The next section provides background and earlier work on force control, visual servoing, and sensor fusion. In Section III, we obtain a new multisensor-based hybrid position/force control law. In Section IV, an image-based visual servoing scheme has been detailed for the purpose of executing a constrained motion on a surface. In Section V, experimental results are described. The paper concludes in Section VI.

II. BACKGROUND AND EARLIER WORK

A. Force Control

The basic hybrid position/force control scheme was originally proposed by Raibert and Craig [47]. It neglected the dynamic coupling effects among each of the robot joints, a problem that was subsequently remedied by Khatib and Burdick [35]. Exact decoupling of motion and force equations and linearization of the resulting system via nonlinear feedback has been accomplished in the *joint space* by Yoshikawa [33] and in the *task space* by McClamroch [38]. In most of the previous work, wherein the end effector made a contact with a surface in the environment, it is assumed that the algebraic constraints imposed on the robot motion are precisely known. In practice, however, the exact location and shape of the surface in Cartesian space is never known precisely. Recently, Wu [40] has proposed a new method for force regulation and contact transition control by using *positive acceleration feedback* but did not study the problem of constrained motion—the main problem that we investigate in this paper.

B. Visual Servoing

Control of robots with visual information is often referred to as *visual servoing*. Early work in visual servoing appeared in late 1970's with the pioneering work of Hill and Park [21] and Weiss *et al.* [20]. Recently, various visual servoing systems have been reported in the literature [8]–[17]. Roughly speaking, the approaches used so far in visual servoing can be classified into two broad categories: position based and image based. In the former approach, a set of images are utilized together with a known camera model to extract the pose of a target in three-dimensional (3-D) space. Subsequently, target tracking is performed by computing the error in the 3-D space as well. On the other hand, in an image-based approach, target tracking is performed by computing the error on the image plane and asymptotically reducing this error to zero. Unfortunately, none of the above two approaches is suitable to establish and maintain contact with a surface, precise position, and orientation of which are unknown. Many of the early research in visual servoing, with the possible exception of Hashimoto [49] and Lei [14], ignored the dynamics of the robot and focused on estimating motion from images or recovering the image Jacobian. In 1993, Papanikolopoulos *et al.* [12] proposed a control model for eye-in-hand system and an adaptive control scheme in which the depth of each individual feature is estimated at each sampling time during execution. In 1994, Castano and Hutchinson [8] introduced a new method called *visual compliance*, a vision-based control scheme that lends itself to task level specification of manipulation goals. Visual compliance is achieved by a hybrid vision/position control structure. Finally, Khosla *et al.* in [13] and [18] proposed control schemes that combine vision and force sensors. A typical implementation proposed is to switch between vision-based and force-based control during different stages of execution. Combining vision and force sensors to achieve real-time tracking in 3-D space, proposed in this

paper, is new. For many other references to visual servoing, the reader is referred to [22]–[30].

C. Sensor Fusion

Sensor fusion, as has been proposed in many earlier studies [3]–[7], is to increase the reliability of the observed sensor data by averaging over redundant sensory measurements. With the development of sensors in the last decade, reliable measurement can now be expected from an individual sensor. Hence sensor redundancy is not required, as it used to be. More recently, a sensor fusion strategy has been proposed by Ishikawa *et al.* [1] to fuse complementary information to obtain inferences that an individual sensor is not able to handle. In this paper, we propose a complementary sensor fusion strategy to fuse force-torque-based and vision-based sensors. For much of the other literature in sensor fusion, the reader is referred to [31]–[54].

III. CONTROL DESIGN

Let us consider a nonredundant rigid robot with six degrees of freedom. As is well known [19], the dynamics of the robot in joint space can be written as

$$D(\mathbf{q})\ddot{\mathbf{q}} + \mathbf{c}(\mathbf{q}, \dot{\mathbf{q}}) + \mathbf{p}(\mathbf{q}) = \tau$$

where $\mathbf{q}$, $\dot{\mathbf{q}}$ and $\ddot{\mathbf{q}} \in \mathbb{R}^6$ are joint angle vector, joint velocity vector, and joint acceleration vector, respectively. $D(\mathbf{q}) \in \mathbb{R}^{6\times6}$ is the inertia matrix of the robot, $\mathbf{c}(\mathbf{q}, \dot{\mathbf{q}})$ stands for coriolis and centrifugal terms, $\mathbf{p}(\mathbf{q})$ is the term caused by gravity, and $\tau \in \mathbb{R}^6$ represents joint torque vector. When the end-effector of the robot makes a contact with a surface in the environment, the dynamics of the robot is given by

$$D(\mathbf{q})\ddot{\mathbf{q}} + \mathbf{c}(\mathbf{q}, \dot{\mathbf{q}}) + \mathbf{p}(\mathbf{q}) = \tau + \mathbf{F} \qquad (3.1)$$

where $\mathbf{F}$ is the constraint force-torque exerted on the joints. The pose of the end-effector in task space and the coordinates of the joint space of the robot are related by

$$(x, y, z, O, A, T)^T = h(\mathbf{q})$$

where (x, y, z) represents position and (O, A, T) represents orientation of the end-effector. By differentiating both sides with respect to time, it turns out that

$$(\dot{x}, \dot{y}, \dot{z}, \dot{O}, \dot{A}, \dot{T})^T = J(\mathbf{q})\dot{\mathbf{q}}$$

where $J(\mathbf{q}) \in \mathbb{R}^{6\times6}$ is the Jacobian of the robot and where the angles O, A, and T have been defined in [55]. Defining $\mathbf{x} = (x, y, z, O, A, T)^T$, we obtain the following dynamics:

$$\dot{\mathbf{x}} = J(\mathbf{q})\dot{\mathbf{q}} \qquad (3.2)$$
$$\ddot{\mathbf{x}} = J(\mathbf{q})\ddot{\mathbf{q}} + \dot{J}(\mathbf{q})\dot{\mathbf{q}}. \qquad (3.3)$$

Throughout this paper, we assume that the dynamics and kinematics of the robot are known.

A. Constrained Motion

In this paper, we assume that the end-effector is initially in contact with the surface. The problem we want to study is how

to move along a suitable trajectory on the surface while maintaining the contact. We also assume that the point of contact between the end-effector and the surface is frictionless. Suppose that the surface is described in the task space as

$$z = z(x, y) \qquad (3.4)$$

where (x, y, z) are coordinates in the task space and $z(x, y)$ is assumed to be smooth. Note that we use the notation (x, y, z) for both "coordinates in the task space" and "position of the end effector." Since the end effector is controlled to remain in contact with the surface, the position coordinates of the end effector can be assumed to satisfy (3.4). While the end-effector maintains contact with the surface, the constrained motion of the robot is given by

$$\dot{z} = \frac{\partial z}{\partial x}\dot{x} + \frac{\partial z}{\partial y}\dot{y}.$$

Writing $G = ((\partial z/\partial x), (\partial z/\partial y), -1, 0, 0, 0)$, we rewrite the constrained motion as

$$G\dot{\mathbf{x}} = 0. \qquad (3.5)$$

Furthermore, differentiating the above constraint, we obtain the following constraint

$$\dot{G}\dot{\mathbf{x}} + G\ddot{\mathbf{x}} = 0. \qquad (3.6)$$

On the other hand, under the assumption that the contact is frictionless, it follows from the principle of virtual work that

$$\mathbf{f}^T\delta\mathbf{x} = \mathbf{F}^T\delta\mathbf{q} = 0 \qquad (3.7)$$

where $\delta\mathbf{x}$ and $\delta\mathbf{q}$ represent the virtual displacements (admissible geometric displacements) of the robot in the task space and the joint space, respectively, and $\mathbf{f}$ is the constraint force exerted on the end-effector in the task space. It follows from (3.7) and (3.2) that

$$\mathbf{F} = J^T\mathbf{f}$$

which describes the relation between the external force exerted on the end-effector to the joint torque and depends upon the geometric structure of the robot.

Since contact is assumed to be made at a point, it follows that

$$\mathbf{f} = (f_x, f_y, f_z, 0, 0, 0)^T. \qquad (3.8)$$

Moreover, for a frictionless contact, the direction of the contact force f is the same as that of G^T, which implies that

$$\mathbf{f} = \lambda G^T \qquad (3.9)$$

for some scalar $\lambda \in \mathbb{R}$.

B. Decoupling of Control Variables

We shall consider the nonlinear feedback control law, given by

$$\tau = \mathbf{c}(\mathbf{q}, \dot{\mathbf{q}}) + \mathbf{p}(\mathbf{q}) + DJ^{-1}\mathbf{u} - DJ^{-1}\dot{J}\dot{\mathbf{q}} \qquad (3.10)$$

where $\mathbf{u}$ is a new control vector to be determined. Substituting the above control torque into the dynamics (3.1) and recalling (3.3) and (3.9), we obtain

$$\ddot{\mathbf{x}} = \mathbf{u} + M^T \lambda \tag{3.11}$$

where

$$M = GJD^{-1}J^T. \tag{3.12}$$

We now define $\Phi = GM^T$ and note that Φ remains a nonzero scalar at all times during the constrained motion since D is nonsingular and G is of full rank. We now define the following two subspaces of $\mathbb{R}^6$.

Definition:

$$S_1(\mathbf{x}) = \{\mathbf{y} \,|\, (I - M^T\Phi^{-1}G)\mathbf{y} = 0, \mathbf{y} \in \mathbb{R}^6\} \tag{3.13}$$
$$S_2(\mathbf{x}) = \{\mathbf{y} \,|\, M^T\Phi^{-1}G\mathbf{y} = 0, \mathbf{y} \in \mathbb{R}^6\}. \tag{3.14}$$

Note that G, M, and Φ are all pose related, and therefore they are functions of x. Note also that the subspaces $S_1(\mathbf{x})$ and $S_2(\mathbf{x})$ are defined for all points on the contact surface (3.4) and that

$$\mathbb{R}^6 = S_1(\mathbf{x}) \oplus S_2(\mathbf{x})$$

where $\oplus$ stands for direct sum. Since M is a nonzero row vector, we obtain $S_2(\mathbf{x}) = \{\mathbf{y} \,|\, G\mathbf{y} = 0, \mathbf{y} \in \mathbb{R}^6\}$. Since G is a nonzero vector, we obtain $\dim(S_2) = 5$ and $\dim(S_1) = 1$.

Premultiplying both sides of (3.11) by G, it follows using (3.6) that

$$\lambda = -\Phi^{-1}(G\mathbf{u} + \dot{G}\dot{\mathbf{x}}). \tag{3.15}$$

If we now asume that $\mathbf{u} = \mathbf{u}_1 + \mathbf{u}_2$ where $\mathbf{u}_1 \in S_1$ and $\mathbf{u}_2 \in S_2$, it follows that $G\mathbf{u}_2 = 0$. Thus we obtain

$$\lambda = -\Phi^{-1}(G\mathbf{u}_1 + \dot{G}\dot{\mathbf{x}}) \tag{3.16}$$

where $\mathbf{u}_1 \in S_1$ and infer that the magnitude λ of the reaction force is controlled only by $\mathbf{u}_1$.

Premultiplying both sides of (3.11) by $(I - M^T\Phi^{-1}G)$ leads to

$$(I - M^T\Phi^{-1}G)\ddot{\mathbf{x}} = (I - M^T\Phi^{-1}G)\mathbf{u}_2$$
$$+ (I - M^T\Phi^{-1}G)M^T\lambda. \tag{3.17}$$

Since $G\mathbf{u}_2 = 0$ and $\Phi = GM^T$, we therefore have

$$(I - M^T\Phi^{-1}G)\ddot{\mathbf{x}} = \mathbf{u}_2 \tag{3.18}$$

where $\mathbf{u}_2 \in S_2$. From (3.18), we infer that $\mathbf{x}$ is controlled by the input $\mathbf{u}_2$, where of course $\mathbf{x}$ is constrained by (3.5).

C. Hybrid Control Laws

At the very outset, we need to choose $\mathbf{u}_1$ to control λ, the magnitude of the force vector, by considering

$$\mathbf{u}_1 = -M^T\left(\lambda^d + K_f \int_{t_0}^t (\lambda^d - \lambda)\,dt\right) - M^T\Phi^{-1}\dot{G}\dot{\mathbf{x}} \tag{3.19}$$

where λ^d is the desired profile that λ is expected to follow and K_f is a suitably chosen constant. It is easy to verify that $\mathbf{u}_1 \in S_1$

since $(I - M^T\Phi^{-1}G)M^T = 0$. Applying the control law (3.19) to (3.16), we obtain

$$(\lambda - \lambda^d) + K_f \int_{t_0}^t (\lambda - \lambda^d)\,dt = 0. \tag{3.20}$$

For a suitable choice of K_f, it follows from (3.20) that $\lim_{t\to\infty} \lambda = \lambda^d$. Hence the choice of $\mathbf{u}_1$ according to (3.19) would asymptotically track the desired λ^d.

We now proceed to compute $\mathbf{u}_2$ in order to control the constrained motion. Note first of all that the constraint (3.5) can be written as

$$f^T\dot{\mathbf{x}} = 0 \tag{3.21}$$

where f is defined in (3.8). The advantage of using (3.21) instead of (3.5) is that f can be measured, whereas G is unknown.

Along the constrained surface, (x, y, z) are not all independent. We therefore define a new state vector $\mathbf{x}_c$ as

$$\mathbf{x}_c = (x \; y \; O \; A \; T)^T \tag{3.22}$$

and note that

$$\dot{\mathbf{x}} = W\dot{\mathbf{x}}_\mathbf{c} \tag{3.23}$$

where

$$W = \begin{bmatrix} 1 & 0 & 0 & 0 & 0 \\ 0 & 1 & 0 & 0 & 0 \\ -\frac{f_x}{f_z} & -\frac{f_y}{f_z} & 0 & 0 & 0 \\ 0 & 0 & 1 & 0 & 0 \\ 0 & 0 & 0 & 1 & 0 \\ 0 & 0 & 0 & 0 & 1 \end{bmatrix}. \tag{3.24}$$

Since G and f are vectors in the same direction, we have

$$\frac{\partial z}{\partial x} = -\frac{f_x}{f_z}, \quad \frac{\partial z}{\partial y} = -\frac{f_y}{f_z}.$$

Hence we compute $GW = 0$. Differentiating (3.23), we obtain

$$\ddot{\mathbf{x}} = W\ddot{\mathbf{x}}_c + \dot{W}\dot{\mathbf{x}}_c. \tag{3.25}$$

From (3.18) and (3.25), we have

$$(I - M^T\Phi^{-1}G)W\ddot{\mathbf{x}}_c + (I - M^T\Phi^{-1}G)\dot{W}\dot{\mathbf{x}}_c = \mathbf{u}_2. \tag{3.26}$$

In order to choose $\mathbf{u}_2$ that would result in a desired trajectory $\mathbf{x}_c^d$ on the constraint surface, we choose

$$\mathbf{u}_2 = W\left[\ddot{\mathbf{x}}_c^d + K_v\left(\dot{\mathbf{x}}_c^d - \dot{\mathbf{x}}_c\right) + K_p\left(\mathbf{x}_c^d - \mathbf{x}_c\right)\right]$$
$$+ (I - M^T\Phi^{-1}G)\dot{W}\dot{\mathbf{x}}_c. \tag{3.27}$$

It is easy to see that $\mathbf{u}_2 \in S_2$ because

$$M^T\Phi^{-1}G\mathbf{u}_2 = M^T\Phi^{-1}G(I - M^T\Phi^{-1}G)\dot{W}\dot{\mathbf{x}}_c = 0$$

in view of the fact that $GM^T = \Phi$. Combining (3.26) and (3.27), we have

$$\ddot{\mathbf{e}}_c + K_v\dot{\mathbf{e}}_c + K_p\mathbf{e}_c = 0 \tag{3.28}$$

where $\mathbf{e}_c = \mathbf{x}_c^d - \mathbf{x}_c$. By choosing K_p and K_v to be a positive number, we ensure that (3.28) is asymptotically stable and hence $\lim_{t\to\infty} \mathbf{e}_c = 0$, $\lim_{t\to\infty} \dot{\mathbf{e}}_c = 0$.
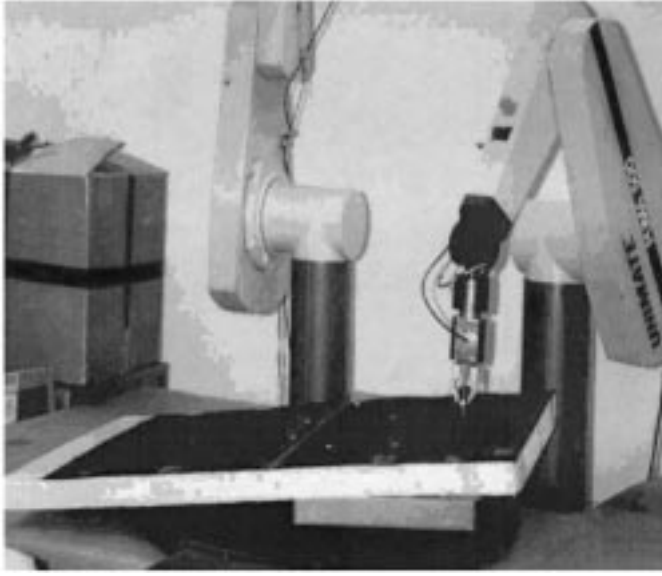
Fig. 3.   Trajectory-following a planar surface.

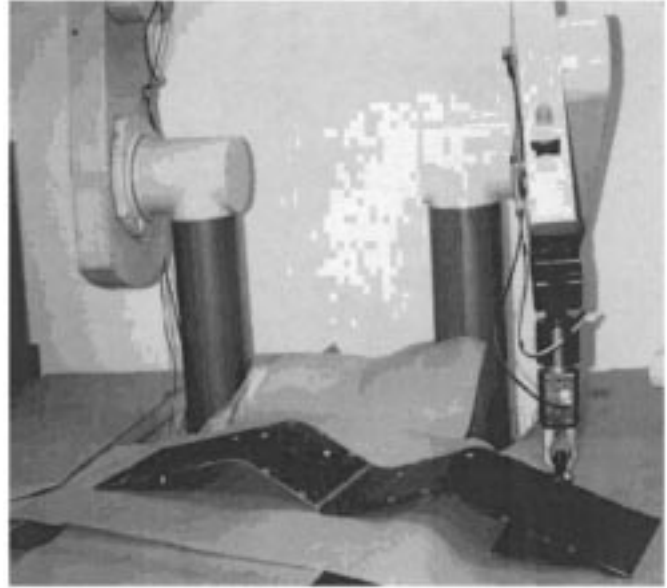
Fig. 4.   Trajectory-following on an unknown surface.

Finally, we combine (3.19) and (3.27) to obtain a hybrid control given by

$$\mathbf{u} = \mathbf{u}_1 + \mathbf{u}_2$$
$$= W\left[\ddot{\mathbf{x}}_c^d + K_v\dot{\mathbf{e}}_c + K_p\mathbf{e}_c\right] + \dot{W}\dot{\mathbf{x}}_c$$
$$- M^T\left[\lambda^d + K_f\int_{t_0}^{d}(\lambda^d - \lambda)\,dt\right]$$
$$- M^T\Phi^{-1}G\dot{W}\dot{\mathbf{x}}_c - M^T\Phi^{-1}\dot{G}\dot{\mathbf{x}}$$

where

$$\dot{G}\dot{\mathbf{x}} = -G\ddot{\mathbf{x}}$$
$$= -GW\ddot{\mathbf{x}}_c - G\dot{W}\dot{\mathbf{x}}_c$$
$$= -G\dot{W}\dot{\mathbf{x}}_c.$$

Hence

$$\mathbf{u} = W\left[\ddot{\mathbf{x}}_c^d + K_v\dot{\mathbf{e}}_c + K_p\mathbf{e}_c\right] + \dot{W}\dot{\mathbf{x}}_c$$
$$- M^T\left[\lambda^d + K_f\int_{t_0}^{t}(\lambda^d - \lambda)\,dt\right] \qquad (3.29)$$

where

$$G = \left[-\frac{f_x}{f_z}, -\frac{f_y}{f_z}, -1, 0, 0, 0\right]$$

and W and M are defined in (3.24) and (3.12), respectively.

The matrix W depends only upon the orientation of the tangent plane to the surface at the point of contact and $\dot{W}$ reflects the change of orientation. For a flat surface as in Fig. 3, $\dot{W} = 0$. The hybrid control (3.29) consists of three parts: The first part is to maintain the position of the end-effector to follow a trajectory on the surface. The second part is to compensate for change in orientation. The last part is to maintain a suitable force on the surface, ensuring contact with the surface at all times. In Fig. 4, we show a nonflat surface where $\dot{W} \neq 0$. The matrix W is a function of the force-torque sensor output and, as will be shown in Figs. 5, 7, and 9, it is noisy. In order to compute $\dot{W}$, one would have to low-pass filter the force measurements by aver-

aging over a time window. Note that the controller only requires the change rate of the direction of the contact force instead of its magnitude. For example, if the contact surface is a plane, there is no change in the direction of the force, even though the magnitude of the force may be noisy. Also, note that in (3.29) the change of the direction of the force only takes effect along with the velocity of the robot $\dot{\mathbf{x}}_c$. If the surface is smooth enough and the speed is not too fast, the effect of the change in force direction is little. Since the paramters W and M can be measured using the force-torque sensor, the controller (3.29) can be implemented provided $\mathbf{x}_c^d$ is known. Unfortunately, since $\mathbf{x}_c^d$ is a curve on an unknown surface, it is not precisely known. In the next section, we handle this problem and replace $\mathbf{x}_c^d$ via the visual sensor.

IV. VISUAL SERVOING OF CONSTRAINED MOTION

In the last section, we showed that the controller (3.29) would control the end effector to asymptotically track a desired trajectory $\mathbf{x}_c^d$ on the surface while continously maintaining contact with the surface. Since $\mathbf{x}_c^d$ is unknown, one would have to recover it using a motion-planning based on a visual sensor. The details are described as follows.

A. Relation Between Constrained Motion and Its Image

Let $(\mathbf{x}_c, \mathbf{y}_c, \mathbf{z}_c)$ and $(\mathbf{x}_b, \mathbf{y}_b, \mathbf{z}_b)$ be the coordinates of a point $\mathbf{p}$ in the camera frame and the base frame of the robot, respectively. The two coordinates are related as follows:

$$\begin{pmatrix} \mathbf{x}_c \\ \mathbf{y}_c \\ \mathbf{z}_c \end{pmatrix} = R\begin{pmatrix} \mathbf{x}_b \\ \mathbf{y}_b \\ \mathbf{z}_b \end{pmatrix} + S \qquad (4.30)$$

where R is a rotation matrix and S is a translation vector. Using a pinhole model of the camera with focal length f, the coordinates of the image of the point $\mathbf{p}$ are given by

$$\begin{pmatrix} \mathbf{x}_{\mathrm{im}} \\ \mathbf{y}_{\mathrm{im}} \end{pmatrix} = \begin{pmatrix} f\frac{\mathbf{x}_c}{\mathbf{y}_c} \\ f\frac{\mathbf{y}_c}{\mathbf{z}_c} \end{pmatrix}. \qquad (4.31)$$
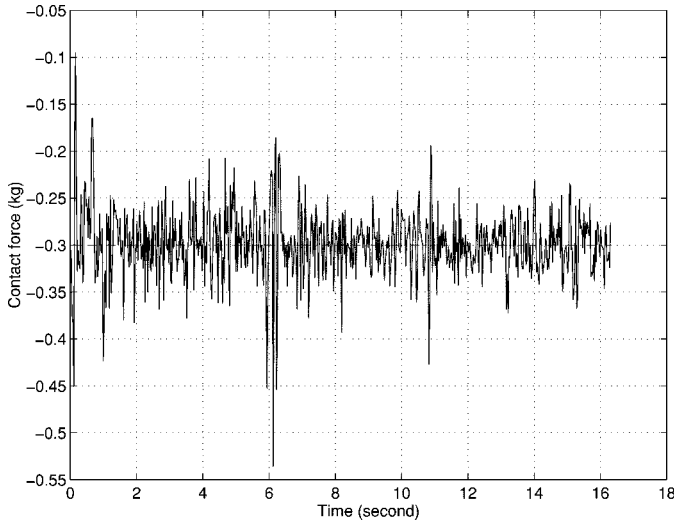
Fig. 5.   Desired and actual contact force for sloped plane.

If $\mathbf{p}$ is a moving point, the optical flow dynamics generated by $\mathbf{p}$ is given by

$$\begin{pmatrix} \dot{\mathbf{x}}_{\mathrm{im}} \\ \dot{\mathbf{y}}_{\mathrm{im}} \end{pmatrix} = \frac{1}{z_c} \begin{pmatrix} f & 0 & -\mathbf{x}_{\mathrm{im}} \\ 0 & f & -\mathbf{y}_{\mathrm{im}} \end{pmatrix} \begin{pmatrix} \dot{\mathbf{x}}_c \\ \dot{\mathbf{y}}_c \\ \dot{\mathbf{z}}_c \end{pmatrix}$$

$$= \frac{1}{\mathbf{z}_c} \begin{pmatrix} f & 0 & -\mathbf{x}_{\mathrm{im}} \\ 0 & f & -\mathbf{y}_{\mathrm{im}} \end{pmatrix} R \begin{pmatrix} \dot{\mathbf{x}}_b \\ \dot{\mathbf{y}}_b \\ \dot{\mathbf{z}}_b \end{pmatrix} \quad (4.32)$$

in view of (4.30). Thus velocity of a moving point with respect to the base frame of a robot generates an optical flow on the image plane described by (4.32). Since the moving point is constrained to the surface (3.4), it follows from (3.21) that

$$\begin{pmatrix} \dot{\mathbf{x}}_b \\ \dot{\mathbf{y}}_b \\ \dot{\mathbf{z}}_b \end{pmatrix} = \begin{pmatrix} 1 & 0 \\ 0 & 1 \\ -\frac{f_x}{f_z} & -\frac{f_y}{f_z} \end{pmatrix} \begin{pmatrix} \dot{\mathbf{x}}_b \\ \dot{\mathbf{y}}_b \end{pmatrix}. \quad (4.33)$$

Combining (4.32) and (4.33), we have

$$\begin{pmatrix} \dot{\mathbf{x}}_{\mathrm{im}} \\ \dot{\mathbf{y}}_{\mathrm{im}} \end{pmatrix} = \frac{1}{\mathbf{z}_c} Q \begin{pmatrix} \dot{\mathbf{x}}_b \\ \dot{\mathbf{y}}_b \end{pmatrix} \quad (4.34)$$

where

$$Q = \begin{pmatrix} f & 0 & -\mathbf{x}_{\mathrm{im}} \\ 0 & f & -\mathbf{y}_{\mathrm{im}} \end{pmatrix} R \begin{pmatrix} 1 & 0 \\ 0 & 1 \\ -\frac{f_x}{f_z} & -\frac{f_y}{f_z} \end{pmatrix}. \quad (4.35)$$

In (4.34), the matrix Q can be computed using vision and force-torque sensor provided we have computed R. By observing the image of the endpoint of the end-effector at various positions in the workspace, the matrix R is estimated using a linear least squares solution. For details of this computation, we refer to [41]. The depth parameter z_c, an unknown, has to be eliminated from (4.34) before applying the least square solution. Subsequently, in this section, we assume that Q can be computed in real time using force-torque and vision sensors.

B. Motion Planning

Assume that $(\mathbf{e}_{x_b} \ \mathbf{e}_{y_b})^T$ is the error vector between the $\mathbf{x}$ and $\mathbf{y}$ coordinates of a point $\mathbf{p}$ on the surface from a desired point $\mathbf{d}$ on the trajectory of the surface, with respect to the base

frame of the robot. Likewise, we assume that $(\mathbf{e}_{x_{\mathrm{im}}} \ \mathbf{e}_{y_{\mathrm{im}}})^T$ is the corresponding error vector on the image plane between the projection of the point $\mathbf{p}$ and the projection of the desired point on the trajectory. We rewrite (4.34) as follows:

$$\begin{pmatrix} \dot{\mathbf{e}}_{x_{\mathrm{im}}} \\ \dot{\mathbf{e}}_{y_{\mathrm{im}}} \end{pmatrix} = \frac{1}{z_c} Q \begin{pmatrix} \dot{\mathbf{e}}_{x_b} \\ \dot{\mathbf{e}}_{y_b} \end{pmatrix} \quad (4.36)$$

and consider the following motion planning:

$$\begin{pmatrix} \dot{\mathbf{e}}_{x_b} \\ \dot{\mathbf{e}}_{y_b} \end{pmatrix} = -kQ^{-1} \begin{pmatrix} \mathbf{e}_{x_{\mathrm{im}}} \\ \mathbf{e}_{y_{\mathrm{im}}} \end{pmatrix} \quad (4.37)$$

where k is chosen to be a constant such that k/z_c is positive at all times. Combining (4.36) and (4.37), we obtain

$$\begin{pmatrix} \dot{\mathbf{e}}_{x_{\mathrm{im}}} \\ \dot{\mathbf{e}}_{y_{\mathrm{im}}} \end{pmatrix} = -\frac{k}{z_c} \begin{pmatrix} \mathbf{e}_{x_{\mathrm{im}}} \\ \mathbf{e}_{y_{\mathrm{im}}} \end{pmatrix} \quad (4.38)$$

which is globally asymptotically stable. Hence

$$\lim_{t \to \infty} (\mathbf{e}_{x_{\mathrm{im}}} \ \mathbf{e}_{y_{\mathrm{im}}}) = 0$$

indicating that asymptotically, the projection of the point $\mathbf{p}$ approaches the projection of the desired trajectory on the image plane and hence $\mathbf{p}$ approaches the desired trajectory on the constrained surface because the end-effector maintains contact with the surface at all times. The magnitude of k remains arbitrary and can be chosen in such a way that the desired velocity of the end-effector remains within an upper and lower limit.

Rewriting the motion planning equation (4.37) in the coordinates of (4.33), we obtain

$$\begin{pmatrix} \dot{x}_b \\ \dot{y}_b \\ \dot{z}_b \end{pmatrix} = -kQ^{-1} \begin{pmatrix} 1 & 0 \\ 0 & 1 \\ -\frac{f_x}{f_z} & -\frac{f_y}{f_z} \end{pmatrix} \begin{pmatrix} \mathbf{e}_{x_{\mathrm{im}}} \\ \mathbf{e}_{y_{\mathrm{im}}} \end{pmatrix}. \quad (4.39)$$

The above motion plan ensures that the robot end-effector is always directed toward the desired point $\mathbf{d}$.

V. EXPERIMENTS

The experimental system consists of one PUMA 560 manipulator, a vision system, and a table on which an unknown surface is placed. The computer vision system consists of a charge-coupled device camera with image resolution of 256×256 and the Intelledex Vision processor based on a 16-MHz Intel 80 386 CPU. The focal length of the camera is 0.0125 m. Our vision system interfaces with the host computer SGI 4D/340 VGX. Visual measurements are sent to SGI by a parallel interface. The robot is controlled by a universal motor controller (UMC) that also interfaces with the SGI through a memory mapping.

In all the experiments, we assume that the relative poses between the camera, table, and robot are unknown and that the unknown surface is either flat or curved. The trajectory to be followed by the end-effector of the robot is characterized by several markers. We adopt our proposed control strategy and control the robot successfully such that the trajectory-following task is completed in a robust manner. Since the proposed method is aimed at an unknown surface, it is robust against uncertainties in the location and shape of the surface. In fact, during the execution of our task, we never need to estimate the shape of the surface *a priori*. Thus our task can be completed even when we assume that the surface is deformable.
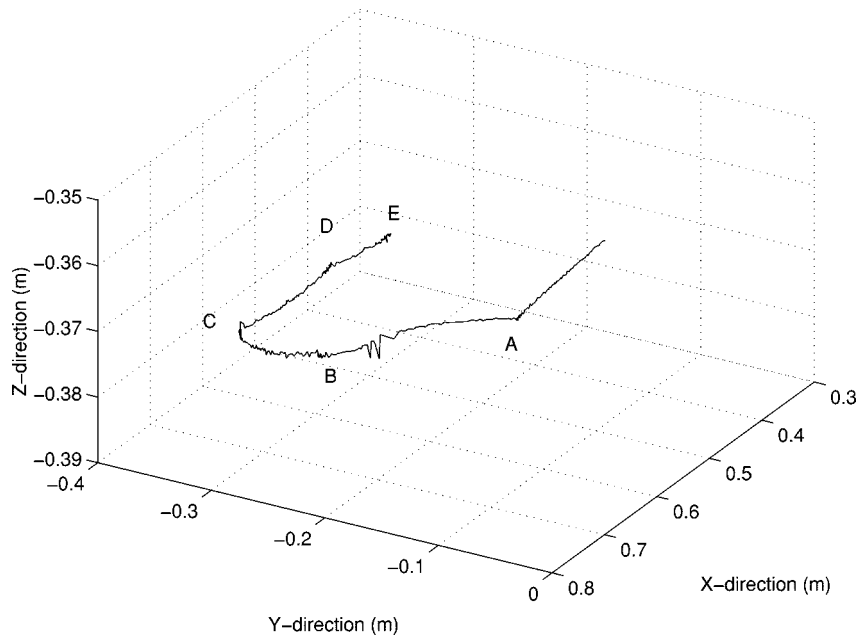
Fig. 6.   Actual trajectory of the end-effector of the robot in the task space for the sloped plane.
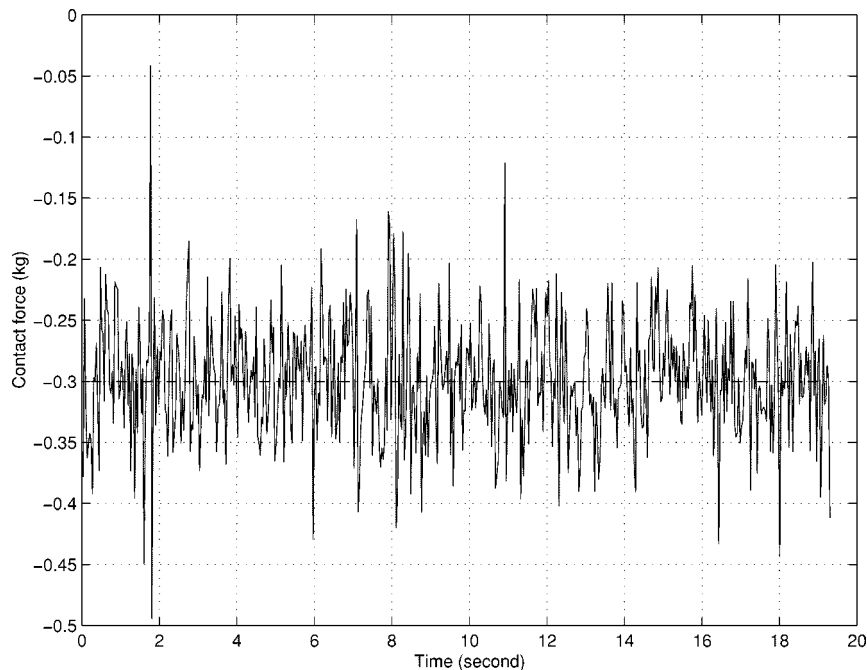

Fig. 7.   Desired and actual contact force when the flat surface is horizontal.

In the experiments performed, we choose $V_{\max} = 0.02$ and $V_{\min} = 0.01$ m/s, the upper and the lower limits of the desired velocity of the end-effector, respectively. We assume that the end-effector initially makes contact with the unknown surface. This is achieved by manually moving the end-effector of the robot to touch the surface. Force control is subsequently used to maintain contact, as has been described earlier. First of all, the robot automatically moves in a predesigned pattern only with the help of force control, while a least squares algorithm is employed to recover the matrix R. In our experiments, this procedure takes about 60 images to process. Once the matrix R is recovered, the robot is automatically controlled to follow the trajectory on the unknown surface. Three subcases has been considered: trajectory-following on a flat surface that is placed horizontally, trajectory-following on a flat surface that has an unknown slope relative to the horizontal plane, and trajectory-following on a curved surface. The flat surface is made of plastic material with foam under it. The curved surface is made of metal. During force control, both the surfaces are assumed to be deformable. Also, we physically reorient the camera to test the feasibility of our algorithm to recover from a lack of calibration data. The results are found to be satisfactory.
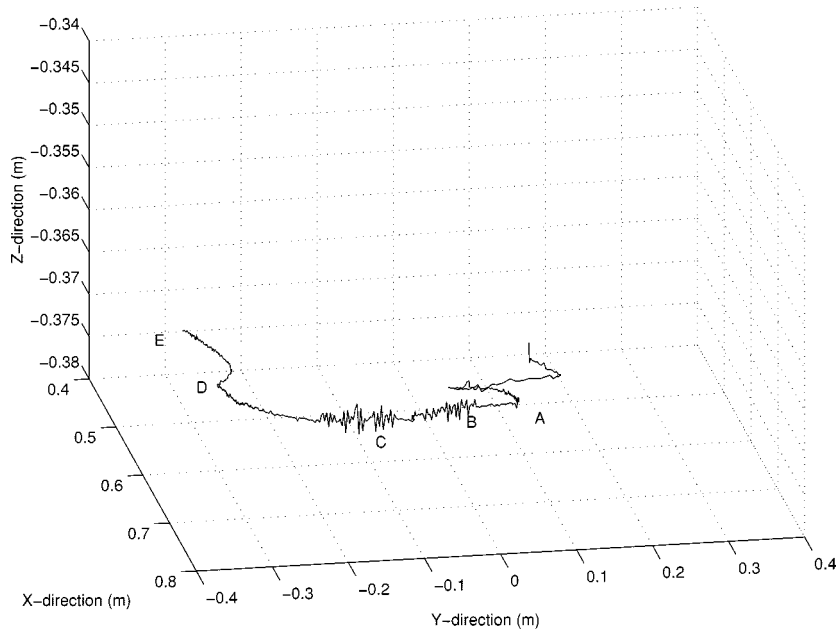
Fig. 8.   Actual trajectory of the end-effector of the robot in the task space when the flat surface is horizontal.
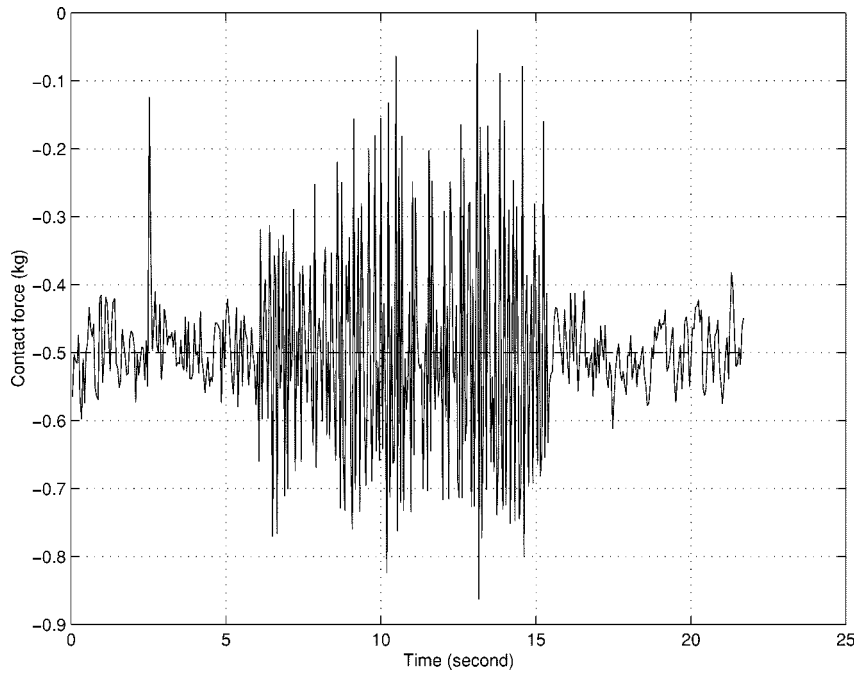

Fig. 9.   Desired and actual contact force for a curved surface.

A. Experimental Results

The experimental results are illustrated in Figs. 5–10. Figs. 5, 7, and 9 show the actual contact force with the desired force being 0.3 (kg) for the flat surface and 0.5 (kg) for the curved surface, respectively, while the actual trajectory of the end-effector of the robot in the task space is given in Figs. 6, 8, and 10, respectively. It should be pointed out that in our experiments, the vision system is able to observe a point on the tool grasped by the end-effector rather than the actual contact point due to poor illumination. In fact, when the image of this point approaches the image of the trajectory on the image plane, the contact point would not be exactly on the required trajectory in the task space. However, in spite of this deficiency, our experiments clearly show the feasibility of our approach.

VI. CONCLUSION

In this paper, we have developed a sensor fusion scheme for controlling an end-effector to follow an unknown trajectory on
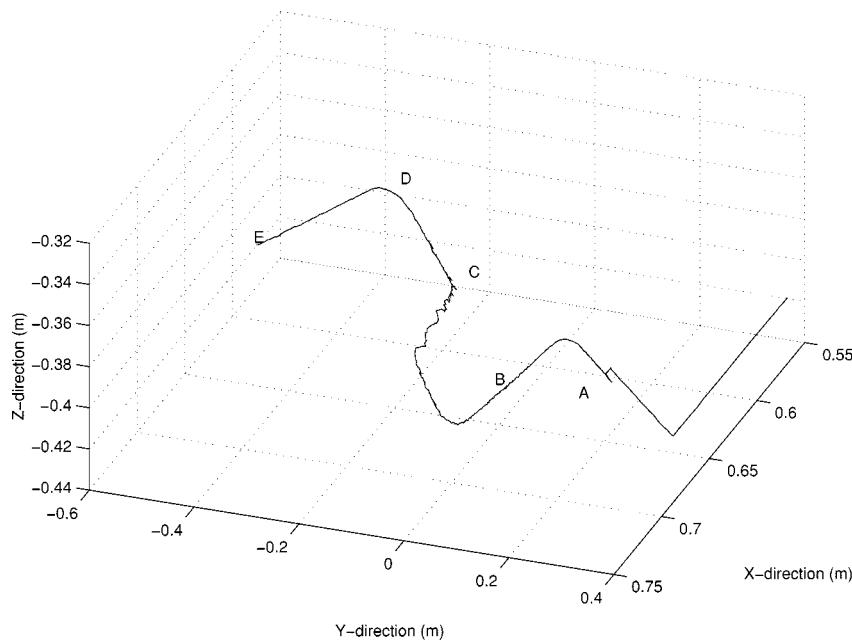
Fig. 10. Actual trajectory of the end-effector of the robot in the task space for a curved surface.

a surface, the position of which is not known *a priori*. At the point of contact, a force-torque sensor mounted on the wrist of the robot provides local information about the unknown surface. The force-torque sensor also provides the necessary control to maintain contact with a desired force on the surface. A vision system, with only one camera, is used to track an unknown trajectory on the surface. The proposed method is robust against calibration parameters that define the position of the camera. The experiments performed have successfully demonstrated the feasibility of the proposed method.

REFERENCES

[1] T. Ishikawa, S. Sakane, T. Sato, and H. Tsukune, "Estimation of contact position between a grasped object and the environment based on sensor fusion of vision and force," in *Proc. IEEE/SICE/RSJ Int. Conf. Multisensor Fusion and Integration for Intelligent Systems*, Washington, DC, Dec. 8–11, 1996, pp. 116–123.

[2] M. J. Magee, B. A. Boyter, C. H. Chien, and J. K. Aggarwal, "Experiments in intensity guided range sensing recognition of three-dimensional objects," *IEEE Trans. Pattern Anal. Machine Intell.*, vol. PAMI-7, Nov. 1985.

[3] Y. Nakamura, *Advanced Robotics: Redundancy and Optimization*. Reading, MA: Addison-Wesley, 1991.

[4] A. Mitiche and J. K. Aggarwal, "Multiple sensor integration/fusion through image processing: A review," *Opt. Eng.*, vol. 25, no. 3, pp. 180–186, 1996.

[5] D. L. Hall, *Mathematical Techniques in Multisensor Data Fusion*. Boston, MA: Artech House, 1992.

[6] R. C. Luo, M. H. Lin, and R. S. Scherp, "The issues and approaches of a robot multi-sensor integration," in *Proc. 1987 IEEE Int. Conf. Robotics and Automation*, Raleigh, NC, 1987, pp. 1941–1946.

[7] A. Flynn, "Redundant Sensors for Mobile Robot Navigation," M.S. thesis, Massachusetts Institute of Technology, Cambridge, July 1985.

[8] A. Castano and S. Hutchinson, "Visual compliance: Task-directed visual servo control," *IEEE Trans. Robot. Automat.*, vol. 10, no. 3, pp. 334–342, 1994.

[9] B. Espiau, F. Chaumette, and P. Rives, "A new approach to visual servoing in robotics," *IEEE Trans. Robot. Automat.*, vol. 8, pp. 313–326, 1992.

[10] J. Feddema, C. Lee, and O. Mitchell, "Weighted selection of image features for resolved rate visual feedback control," *IEEE Trans. Robot. Automat.*, vol. 7, pp. 31–47, 1991.

[11] W. Wilson, "Visual servo control of robots using Kalman filter estimates of robot pose relative to work-pieces," in *Visual Servoing*, K. Hashimoto, Ed. Singapore: World Scientific, 1994, pp. 71–104.

[12] N. Papanikolopoulos, P. K. Khosla, and T. Kanade, "Visual tracking of a moving target by a camera mounted on a robot: A combination of control and vision," *IEEE J. Robot. Automat.*, vol. 9, pp. 14–35, 1993.

[13] N. P. Papanikolopoulos and P. K. Khosla, "Robotic visual servoing around a static target: An example of controlled active vision," in *Proc. 1992 American Control Conf.*, Chicago, IL, 1992, pp. 1489–1494.

[14] M. Lei, "Vision Based Robot Tracking and Manipulation," D.Sc. dissertation, Washington Univ., May 1994.

[15] B. Nelson and P. K. Khosla, "Increasing the tracking region of an eye-in-hand system by singularity and joint limit avoidance," in *Proc. IEEE Int. Conf. Robotics and Automation*, Piscataway, NJ: IEEE Computer Society Press,, 1993, pp. 418–423.

[16] A. J. Koivo and N. Houshangi, "Real-time vision feedback for servoing of a robotic manipulator with self-tuning controller," *IEEE Trans. Syst., Man, Cybern.*, vol. 21, pp. 134–142, Jan. 1991.

[17] P. K. Allen, B. Yoshimi, and A. Timcenko, "Real-time visual servoing," in *Proc. IEEE Int. Conf. Robotics and Automation*, 1991, pp. 851–856.

[18] B. J. Nelson and P. K. Khosla, "Force and vision resolvability for assimilating disparate sensory feedback," *IEEE J. Robot. Automat.*, vol. 12, pp. 714–731, Oct. 1996.

[19] T. J. Tarn, A. K. Bejczy, A. Isidori, and Y. Chen, "Nonlinear feedback in robot arm control," in *Proc. 23rd IEEE Conf. Decision and Control*, Las Vegas, NV, 1984, pp. 736–751.

[20] L. Weiss, A. Sanderson, and C. Neuman, "Dynamic sensor based control of robots with visual feedback," *IEEE J. Robot. Automat.*, vol. RA-3, pp. 404–417, Oct. 1987.

[21] J. Hill and W. T. Park, "Real time control of a robot with a mobile camera," in *Proc. 9th ISIR*, Washington, DC, Mar. 1979, pp. 233–246.

[22] E. D. Dickmanns and V. Graefe, "Dynamic monocular machine vision," *Machine Vision Applicat.*, vol. 1, pp. 223–240, 1988.

[23] J. T. Feddema and O. R. Mitchell, "Vision-guided servoing with feature-based trajectory generation," *IEEE J. Robot. Automat.*, vol. 5, pp. 691–700, Oct. 1989.

[24] P. I. Corke, "Visual control of robot manipulators—A review," in *Visual Servoing*, K. Hashimoto, Ed, Singapore: World Scientific, 1994, pp. 1–32.

[25] Z. Zhang, Q. T. Luong, and O. Faugeras, "Motion of an uncalibrated stereo rig: Self-calibration and metric reconstruction," *IEEE Trans. Robot. Automat.*, vol. 12, no. 1, pp. 103–113, 1996.

[26] S. D. Ma, "A self-calibration technique for active vision systems," *IEEE Trans. Robot. Automat.*, vol. 12, no. 1, pp. 114–120, 1996.

[27] "Special section on vision-based control of robot manipulators," *IEEE Trans. Robot. Automat.*, vol. RA-12, no. 5, 1996.

[28] "Modeling issues in visual sensing," *Math. Comput. Modeling*, vol. 24, no. 5, 6, 1996.

[29] G. D. Hager, "A modular system for robust positioning using feedback from stereo vision," *IEEE Trans. Robot. Automat.*, vol. 13, no. 4, pp. 582–595, 1997.

[30] S. Hutchinson, G. D. Hager, and P. I. Corke, "A tutorial on visual servo control," *IEEE Trans. Robot. Automat.*, vol. 12, no. 5, pp. 651–670, 1996.

[31] B. H. Yoshimi and P. K. Allen, "Alignment using an uncalibrated camera system," *IEEE Trans. Robot. Automat.*, vol. 11, no. 4, pp. 516–521, 1995.

[32] D. E. Whitney, "Force feedback control of manipulator fine motions," *ASME J. Dynamic Syst. Measure. Control*, vol. 99, no. 2, pp. 91–97, 1977.

[33] T. Yoshikawa, "Dynamic hybrid position/force control of robot manipulators—Description on hand constraint and calculation of joint driving force," in *Proc. IEEE Int. Conf. Robot. Automat.*, 1986, pp. 1393–1398.

[34] T. Yoshikawa and A. Sudou, "Dynamic hybrid position/force control of robot manipulators-on-line estimation of unknown constraint," *IEEE Trans. Robot. Automat.*, vol. 9, no. 2, pp. 220–226, 1993.

[35] O. Khatib and J. Burdick, "Motion and force control of robot manipulators," in *Proc. IEEE Int. Conf. Robotics and Automation*, 1986, pp. 1381–1386.

[36] M. T. Mason, "Compliance and force control for computer controlled manipulators," *IEEE Trans. Syst., Man, Cybern.*, vol. SMC-11, pp. 418–431, Nov. 1981.

[37] J. E. Slotine and W. Li, "Adaptive strategies constrained manipulation," in *Proc. IEEE Int. Conf. Robotics and Automation*, 1987, pp. 595–601.

[38] N. H. McClamroch, "Singular systems of differential equations as dynamic models of constrained robot systems," in *Proc. IEEE Int. Conf. Robotics and Automation*, 1986, pp. 21–28.

[39] H. Bruyninckx and J. De Schutter, "Specification of force-controlled actions in the "task frame formalism"—A synthesis," *IEEE J. Robot. Automat.*, vol. 12, pp. 581–589, 1996.

[40] Y. Y. Wu, "Force regulation and contact transition control," D.Sc. dissertation, Washington Univ., May 1996.

[41] D. Xiao, "Multisensor based robotic manipulation in uncalibrated environments," D.Sc. dissertation, Washington Univ., May 1997.

[42] R. P. Paul and B. Shimano, "Compliance and control," in *Proc. Joint Automatic Control Conf.*, 1976, pp. 694–699.

[43] K. Y. Lim and M. Eslami, "Robust adaptive controller designs for robot manipulator systems," *IEEE J. Robot. Automat.*, vol. RA-3, pp. 54–66, 1987.

[44] M. H. Ozaki and M. Takata, "On the force feedback control of a manipulator with a compliant wrist force sensor," *Mechanism Machine Theory*, vol. 18, no. 1, pp. 57–62, 1986.

[45] H. Van Brussel and J. Simons, "Robot assembly by active force feedback accommodation," *Manufact. Technol. CIRP Annals*, vol. 28, no. 1, pp. 397–401, 1979.

[46] J. K. Salisburg, "Active stiffness control of a manipulator in Cartesian coordinates," in *Proc. 19th IEEE Conf. Decision and Control*, 1980, pp. 95–100.

[47] M. H. Raibert and J. J. Craig, "Hybrid position/force control of manipulators," *ASME J. Dynam. Syst., Measure. Control*, vol. 103, no. 2, pp. 126–133, 1981.

[48] N. Hogan, "Impedance control; An approach to manipulation: Part I—Theory; Part II—Implementation; Part III—Applications," *ASME J. Dynam. Syst., Measure. Control*, vol. 107, pp. 1–24, 1985.

[49] K. Hashimoto, "LQ optimal and nonlinear approaches to visual servoing," in *Visual Servoing*, K. Hashimoto, Ed, Singapore: World Scientific, 1994, pp. 165–198.

[50] P. K. Allen, A. T. Miller, P. Y. Oh, and B. S. Leibowitz, "Integration of vision and force sensors for grasping," in *Proc. IEEE/SICE/RSJ Int. Conf. Multisensor Fusion and Integration for Intelligent Systems*, Washington, DC, Dec. 8–11, 1996, pp. 349–356.

[51] B. K. Ghosh, D. Xiao, N. Xi, and T. J. Tarn, "Multisensor based robotic manipulation in an uncalibrated manufacturing workcell," *J. Franklin Inst.*, vol. 336, no. 2, pp. 237–255, 1999.

[52] ——, "Integration of real-time planning and control in an unstructured manufacturing workcell," *Adv. Robot. J.*, to be published.

[53] P. K. Allen, "Integrating vision and touch for object recognition tasks," *Int. J. Robot. Res.*, vol. 7, no. 6, pp. 15–33, 1988.

[54] S. A. Stansfield, "A robotic perceptual system utilizing passive vision and active touch," *Int. J. Robot. Res.*, vol. 7, no. 6, pp. 138–161, 1988.

[55] T. J. Tarn, A. K. Bejczy, and G. T. Marth, "Kinematic Characterization of the PUMA 560 manipulator," Dept. Syst. Sci. Math., Washington Univ., Saint Louis, MO, Robotics Laboratory Rep. SSM-RL-91-15, Dec. 1991.

Di Xiao received the B.S. degree in mechanical engineering and the M.S. degree in control theory and applications from Beijing University of Aeronautics and Astronautics, China, in 1984 and 1989, respectively, and the D.Sc. degree in systems science and mathematics from Washington University, St. Louis, MO, in 1997.

During 1989–1993, he was with Beijing University of Aeronautics and Astronautics. Since September 1997, he has been with Fanuc Robotics North America, Inc. His research interests include motion planning, control theory, and applications.

Bijoy K. Ghosh :(A'78–S'79–M'83–SM'90–F'00) received the bachelor's degree in electrical and electronics engineering from Birla Institue of Technology and Sciences, Pilani, India, in 1977, the master's degree in electrical engineering from the Indian Institute of Technology, Kanpur, India, in 1979, and the Ph.D. degree in engineering from the Decision and Control Group of the Division of Applied Sciences, Harvard University, Cambridge, MA, in 1983.

Since 1983, he has been a Professor in the Systems, Science and Mathematics Department at Washington University, St. Louis, MO, and Director of the center for BioCybernetics and Intelligent Systems with research interests in the areas of multivariable control theory, biological and machine vision, robotic manufacturing, and neural engineering. He was a Visiting Fellow at Osaka University and the Tokyo Institute of Technology during 1992 and 1995, respectively. In 1993, he was the United Nations Development Program Fellow under the TOKTEN program and visited the Indian Institute of Technology, Kharagpur. In 1997, he received the Japan Society for the Promotion of Science invitation fellowship for research in Japan and visited Tokyo Denki University. He was the Program Chair for the International Conference on Multisensor Fusion and Integration, 1999.

Dr. Ghosh is Chairman for the technical committee on Sensor Guided Manipulation in Automation in the IEEE Robotics and Automation Society. In 1988, he received the American Automatic Control Council's Donald P. Eckman Award in recognition of his outstanding contribution in the field of automatic control.

Ning Xi received the B.S. degree in electrical engineering from Beijing University of Aeronautics and Astronautics, China, the M.S. degree in computer science from Northeastern University, Boston, MA, and the D.Sc. degree in systems science and mathematics from Washington University, St. Louis, MO, in 1993.

Currently, he is an Assistant Professor in the Department of Electrical and Computer Engineering, Michigan State University, East Lansing. His current research interests include robotics, manufacturing automation, intelligent control, and systems.

Prof. Xi received the Excellent Research Award from the Japan Foundation for the Promotion of Advanced Automation Technology in March 1995. He received the Best Paper Award at the IEEE/RSJ International Conference on Intelligent Robots and Systems in August 1995 and the first Early Academic Career Award from the IEEE Robotics and Automation Society in May 1999. He received a National Science Foundation CAREER Award.

T. J. Tarn (M'71–Sm'83–F'85) received the D.Sc. degree in control system engineering from Washington University, St. Louis, MO.

He is currently a Professor in the Department of Systems Science and Mathematics and Director of the Center for Robotics and Automation at Washington University.

He was President of the IEEE Robotics and Automation Society during 1992–1993, Director of IEEE Division X (Systems and Control) during 1995–1996, and a member of the IEEE Board of Directors during 1995–1996. At present, he is a member of the Nomination Committee of the IEEE Board of Directors. He is Chairman of the Management Committee and an Editor of the IEEE/ASME TRANSACTIONS ON MECHATRONICS. He is a board member of the IEEE Neural Network Council. He received the NASA Certificate of Recognition for the creative development of a technical innovation on robot arm dynamic control by computer in 1987. The Japan Foundation for the Promotion of Advanced Automation Technology presented him with the Best Research Article Award in March 1994. He also received the Best Paper Award at the 1995 IEEE/RSJ International Conference on Intelligent Robots and Systems and the Distinguished Member Award from the IEEE Control Systems Society in 1996. He is the first recipient of both the Nakamura Prize (in 1997) and the Ford Motor Company Best Paper Award at the Japan/US Symposium on Flexible Automation (in 1998). In addition, he was featured in the "Special Report on Engineering" of the "1998 Best Graduate Schools" issue of *US News and World Report*.